
Reviving Stale Updates: Data-Free Knowledge Distillation for Asynchronous Federated Learning

Baris Askin^{1,*},[†]
Carlee Joe-Wong¹

Holger R. Roth²
Gauri Joshi¹

Zhenyu Sun^{3,*}
Ziyue Xu²

¹Carnegie Mellon University

²NVIDIA

³Northwestern University

Abstract

Federated Learning (FL) enables collaborative model training across distributed clients without sharing raw data, yet its scalability is limited by synchronization overhead. Asynchronous Federated Learning (AFL) alleviates this issue by allowing clients to communicate independently, thereby improving wall-clock efficiency in large-scale, heterogeneous environments. However, this asynchrony introduces stale updates (client updates computed on outdated global models) that can destabilize optimization and hinder convergence. We propose FEDREVIVE, an asynchronous FL framework that revives stale updates through data-free knowledge distillation (DFKD). FEDREVIVE integrates parameter-space aggregation with a lightweight, server-side DFKD process that transfers knowledge from stale client models to the current global model without access to real or public data. A meta-learned generator synthesizes pseudo-samples, which enables multi-teacher distillation. A hybrid aggregation scheme that combines raw updates with DFKD updates effectively mitigates staleness while retaining the scalability of AFL. Experiments on various vision and text benchmarks show that FEDREVIVE achieves faster training up to 32.1% and higher final accuracy up to 21.5% compared to asynchronous baselines.

concerns about privacy and regulatory compliance (Yang et al., 2019). Federated Learning (FL) addresses this dilemma by enabling many clients (e.g., smartphones, wearables, hospital servers) to collaboratively train a shared model without uploading raw data (McMahan et al., 2017). In vanilla FL, the server broadcasts the current global model, each selected client performs local training on private data, and the server aggregates returned updates to form the next global iterate (McMahan et al., 2017). This paradigm preserves data locality and widens access to otherwise restricted data, while also reducing central storage risks. At the same time, relying only on public datasets is increasingly insufficient, as web-scale models steadily saturate accessible corpora and demand broader coverage across modalities and domains. FL serves both cross-silo deployments (e.g., hospitals and enterprises) and cross-device settings with millions of intermittently available phones, providing a practical path to leverage diverse private data at scale (Rieke et al., 2020; Lai et al., 2021).

In *synchronous* FL, the server waits for all (or a selected subset of) participating clients to complete their local updates before aggregating them into a new global model (McMahan et al., 2017). Although this strategy ensures that all updates are aligned to the same global state, it suffers from the well-known *straggler problem*, which is that slow or unavailable clients delay the entire round, leading to underutilized resources and poor scalability when client availability or compute capacity varies (Xie et al., 2019).

Asynchronous FL (AFL) alleviates this bottleneck by allowing the server to immediately incorporate each client’s update upon arrival, without waiting for others (Xie et al., 2019; Nguyen et al., 2022). Thus, clients train and communicate independently, and the server continuously updates the global model. This property significantly improves wall-clock efficiency and makes AFL particularly appealing for cross-device scenarios with thousands of mobile or edge participants and for

1 Introduction

Modern artificial intelligence (AI) models thrive on large amounts of data, which raises serious

*Work was done during an internship at NVIDIA.

[†]Corresponding author.

cross-silo collaborations where institutional availability fluctuates. The removal of synchronization barriers enables better utilization of communication and computation resources, leading to faster overall convergence in wall-clock time.

The flexibility of AFL, however, comes with a major drawback. Since clients train on potentially outdated versions of the global model, the server often aggregates *stale updates* computed with respect to earlier global states. Such staleness can distort optimization dynamics and degrade model performance, especially under heterogeneous or non-IID (non-independent and identically distributed) data distributions (Xie et al., 2019; Nguyen et al., 2022; Askin et al., 2024; Richtarik, 2025). Despite this, stale updates are not purely detrimental; they encapsulate valuable information about local data of clients. The fundamental challenge is how to effectively exploit this informative content without exacerbating the drift caused by delayed updates. Therefore, we ask:

*Can we **revive** stale updates in asynchronous FL to extract useful knowledge for improved scalability?*

Our idea: Distill knowledge from stale updates.

We answer the question by combining parameter-space aggregation with *data-free knowledge distillation*. Knowledge distillation (KD) transfers information from one or more teachers to a student using softened targets or intermediate features (Hinton et al., 2015). Data-free variants (DFKD) avoid the assumption of a public data availability (Lopes et al., 2017a), which aligns with practical conditions in FL. Integrating KD into AFL, however, introduces unique challenges: (i) no shared or public data are typically available for distillation, (ii) stale client models may be poor or heterogeneous teachers, and (iii) the distillation process must remain lightweight to preserve AFL’s scalability advantage. Our approach addresses these issues and exploits the informative content of stale updates in a data-free manner to improve global model quality without sacrificing asynchrony.

Contributions. The main contributions of the paper are summarized as follows:

- We propose FEDREVIVE, an AFL framework that *revives* stale client updates by combining parameter aggregation with server-side, multi-teacher DFKD.
- We carefully design a DFKD pipeline, tailored to AFL. We leverage a multi-teacher distillation with computation-light process to operationalize our idea.
- We demonstrate improved scalability and accuracy over the baseline methods under realistic simulations

with image and text-domain experiments, achieving faster time-to-target accuracy and better final performance.

Our results indicate that stale client updates still carry rich, transferable knowledge. By extracting that knowledge in a data-free manner and fusing it with parameter-space aggregation, AFL can retain its scalability advantages without sacrificing model quality.

2 Related Work

Synchronous FL. Since the seminal work of McMahan et al. (2017), FL has proven effective for collaboratively training models from decentralized and private data sources. Most existing FL algorithms employ *synchronous* aggregation, where the server waits for all selected clients to complete their local training and then averages their model updates. However, this synchronization scheme creates a major bottleneck. In realistic environments, edge devices exhibit high variability in computation and communication capabilities (e.g., mobile phones versus embedded edge devices, Wi-Fi versus cellular connections), resulting in widely varying local training times. Consequently, in each round, the server must wait for the slowest client (the “straggler”), leaving faster clients idle and underutilized. Several methods have been proposed to alleviate the straggler problem, such as aggregating only the updates that arrive before a predetermined time (Bonawitz et al., 2019) or randomly subsampling available clients (Luo et al., 2022). However, these approaches can bias training toward inherently faster clients and still underutilize slower ones. The straggler issue is further exacerbated in large-scale deployments, where the growing number of clients increases the likelihood of slow update returns and communication delays (Yu et al., 2023). As a result, synchronous aggregation inherently limits scalability and resource efficiency in federated networks.

Asynchronous FL. To overcome the straggler bottleneck and scalability issues of synchronous aggregation, a growing body of work has explored *asynchronous FL* (AFL) (Xie et al., 2019; Xu et al., 2023; Nguyen et al., 2022; Chen et al., 2020; Richtarik, 2025; Nichol et al., 2018). AFL builds upon a line of previous works on asynchronous distributed stochastic gradient descent (SGD) in the data-center setting (Dean et al., 2012; Gupta et al., 2016; Cui et al., 2014; Ho et al., 2013; Lian et al., 2015; Zhang et al., 2016; Mitliagkas et al., 2016; Dutta et al., 2018). In AFL, the server integrates client updates as soon as they arrive, either individually or in small mini-batches, without waiting for global synchronization. This design enables faster convergence by mitigating the straggler effect and im-

proving resource utilization. However, asynchronicity introduces a new challenge: *stale updates*. Because clients train on outdated versions of the global model, their updates may become obsolete by the time they reach the server. Incorporating these stale updates can inject inconsistency or even destabilize training (Xu et al., 2023).

To mitigate staleness, several strategies have been proposed. Nguyen et al. (2022) employ buffer for incoming updates and averages them before aggregation, which smooths model update frequency and reduces variance within the server updates due to data heterogeneity despite the cost of slower server updates. Another line of work assigns lower weights to stale updates as a function of their staleness (Chen et al., 2019; Shi et al., 2020; Lu et al., 2020; Zhang et al., 2016; Dutta et al., 2018; Cui et al., 2014), reducing the influence of outdated gradients but potentially discarding valuable information from slower clients. Importantly, each client’s update encapsulates rich information about its local data distribution. In AFL, the challenge lies in how to effectively utilize this information despite staleness. In our work, we leverage DFKD to extract and transfer the informative content from stale client updates to the current server model.

KD and DFKD. KD is a powerful technique for transferring learned representations of a better-performing *teacher* model to a *student* (Hinton et al., 2015). The standard formulation trains the student to mimic the teacher’s output logits, which encode class probabilities, inter-class similarity, and uncertainty. KD has since been widely adopted across various modalities, including vision, speech, and natural language processing, where it consistently improves generalization and model compactness (Mansourian et al., 2025; Zagoruyko and Komodakis, 2017; Jiao et al., 2020). The vanilla KD framework, however, fundamentally requires access to a dataset on which both teacher and student are evaluated during distillation. In many practical cases, such as privacy-preserving learning or FL, direct access to data is unavailable, making conventional KD infeasible. This has motivated the emergence of DFKD (Lopes et al., 2017b), which aims to perform distillation without real data. Methods typically optimize a generator or latent codes to synthesize pseudo-samples under objectives that align teacher predictions, match intermediate statistics (e.g., batch statistics), or introduce adversarial criteria to amplify teacher–student discrepancies (Mansourian et al., 2025; Lopes et al., 2017b; Fang et al., 2022). Then, these samples are utilized for distillation.

KD and DFKD in FL. KD has also been incorporated into the FL paradigm for various purposes,

such as mitigating client bias and data heterogeneity, enabling architecture-heterogeneous models, and enhancing data privacy (Li et al., 2024; Li and Wang, 2019; Lin et al., 2020; Qin et al., 2024; Fan et al., 2024). In FL, KD can be performed on either the *server side*, where the global model distills knowledge from client models (Lee et al., 2020; Li and Wang, 2019), or on the *client side*, where clients distill knowledge from the server model or peer models (Itahara et al., 2021; Shang et al., 2023). While some of these methods assume the presence of a shared public dataset for knowledge transfer (Itahara et al., 2021), some approaches adopt *DFKD* to remove this dependency (Gao et al., 2025; Zhang et al., 2022; Zhu et al., 2021). However, existing works applying KD or DFKD have been primarily designed for *synchronous* FL, and the use of KD in *asynchronous* FL remains largely unexplored. The few existing efforts (Lu et al., 2025) rely on the unrealistic assumption of public data availability. In this work, we leverage DFKD in the asynchronous FL setting to enhance both scalability and convergence stability.

3 FL Problem & Method

Problem formulation. We consider an FL setup with N clients collaboratively optimizing a shared global model \mathbf{x} . Each client i has its own local objective function $f_i(\mathbf{x})$, defined by its private data. The local objectives f_i differ across clients due to the heterogeneity in data distribution. The aim is to minimize a global learning objective, formulated as the average of local losses:

$$F(\mathbf{x}) = \frac{1}{N} \sum_{i \in [N]} f_i(\mathbf{x}) \quad (1)$$

Asynchronous framework. We first describe a generic AFL framework that encompasses both existing asynchronous schemes (Xie et al., 2019; Nguyen et al., 2022) and our proposed method FEDREVIVE. The overall process is summarized in Algorithm 1. After initialization (line 2), the server processes and aggregates each of the received updates and assigns a new client for local training, repeating these steps until convergence (lines 4 - 7). The key difference between AFL variants lies in the *aggregation step* (line 6), where the server integrates the received client update into the global model. The client local training, consisting of multiple steps of updates with a selected optimizer and stochastic gradients, is also depicted in Algorithm 1.

Vanilla and buffered AFL. The *vanilla* AFL algorithm (Xie et al., 2019) updates the global model immediately when an update arrives from a client. Ac-

Algorithm 1 Generic AFL Framework

Server Process:

- 1: **Inputs:** Initial model $\mathbf{x}^{(0)}$, server and client learning rates η_s and η_c , #local iterations K , #rounds T , #selected active clients N_a .
- 2: Send $\mathbf{x}^{(0)}$ to N_a randomly selected active clients.
- 3: **for** $t = 0$ **to** $T - 1$ **do**
- 4: **Wait** until the server receives an τ_i^t -stale updated model $\tilde{\mathbf{x}}_i^{(t-\tau_i^t)}$ from client i .
- 5: Client update $\Delta_i^{(t-\tau_i^t)} \leftarrow \tilde{\mathbf{x}}_i^{(t-\tau_i^t)} - \mathbf{x}^{(t-\tau_i^t)}$.
- 6: **Process update using one of Eqs (2), (3), or (4).**
- 7: Assign local training to a randomly selected active client with the updated model $\mathbf{x}^{(t+1)}$.
- 8: **end for**

Client i 's Local Training (Async. and Parallel):

- 9: **Input:** Received server model \mathbf{x} .
- 10: Initialize $\tilde{\mathbf{x}} \leftarrow \mathbf{x}$.
- 11: **for** $k = 1$ **to** K **do**
- 12: $\tilde{\mathbf{x}} \leftarrow \tilde{\mathbf{x}} - \eta_c \tilde{\nabla} f_i(\tilde{\mathbf{x}})$ {A stoch. grad. update}
- 13: **end for**
- 14: **Return** $\tilde{\mathbf{x}}$ to the server.

cordingly, the aggregation step in Algorithm 1 (line 6) becomes:

$$\mathbf{x}^{(t+1)} \leftarrow \mathbf{x}^{(t)} + \eta_s \Delta_i^{(t-\tau_i^t)} \quad (2)$$

Each time the server updates \mathbf{x} , the staleness of the ongoing local trainings implicitly increases by one, since these clients' local models are now further outdated. This simple yet effective scheme eliminates the need for synchronization but often leads to unstable training and divergence when τ_i^t grows large. FEDBUFF (Nguyen et al., 2022) introduces a buffering mechanism that accumulates multiple updates before aggregation. Specifically, the server maintains a buffer \mathcal{B} of size B to average updates and aggregate them when B updates are received. The aggregation step in Algorithm 1 (line 6) becomes:

$$\begin{aligned} &\mathcal{B} \leftarrow \mathcal{B} \cup \{\Delta_i^{(t-\tau_i^t)}\} \\ &\text{if } |\mathcal{B}| = B : \\ &\quad \mathbf{x}^{(t+1)} \leftarrow \mathbf{x}^{(t)} + \frac{\eta_s}{B} \sum_{\Delta \in \mathcal{B}} \Delta, \text{ and set } \mathcal{B} \leftarrow \emptyset \quad (3) \\ &\text{else: } \mathbf{x}^{(t+1)} \leftarrow \mathbf{x}^{(t)} \end{aligned}$$

This buffered strategy smooths the staleness effect by

reducing the update frequency. However, as the buffer size B increases, the infrequent server model updates slow down the training. Our method, FEDREVIVE, described next, mitigates the staleness without reducing the server model update frequency, thus enabling faster training.

3.1 Overview of FedRevive

Motivation. In AFL, the most critical challenge is *update staleness* (Xie et al., 2019), which leads to training instability and poor convergence. Since the staleness increases with the number of participating clients (Koloskova et al., 2022), the scalability of FL and large-scale deployments are limited. In our paper, we define the staleness of an update as the number of server updates between when a client starts local training and when its update is received at the server (Koloskova et al., 2022; Chen et al., 2021; Askin et al., 2024). Denoting the global model by \mathbf{x} and a client update by Δ , in server round t , the server may receive a τ_i^t -stale update $\Delta_i^{(t-\tau_i^t)}$ from client i , indicating that the client trained on an earlier model $\mathbf{x}^{(t-\tau_i^t)}$. Conventional FL methods rely on parameter space aggregation, adding Δ scaled by a learning rate to \mathbf{x} (Wang et al., 2020; McMahan et al., 2017). However, this can cause severe inconsistency due to stale and current model versions, destabilizing training and degrading performance. Yet, even stale updates encapsulate rich information about the client's private data, which we would like to incorporate into the global model. To meet these goals, our key idea is to leverage KD to extract and transfer informative knowledge from the stale update to the current server model. By coupling parameter space updates with a KD-guided update, our method mitigates the adverse effects of staleness. In our KD framework (more details in Section 3.2), the client's locally updated model serves as a teacher while the current server model is the student.

FedRevive aggregation. In our proposed method, FEDREVIVE, the server adaptively fuses the conventional parameter-space update with a knowledge-distilled update to alleviate the adverse effect of staleness. When the server receives a τ_i^t -stale client update $\Delta_i^{(t-\tau_i^t)}$, it first obtains a knowledge-distilled update through a data-free distillation process. The server then combines the original parameter update and the KD-based update through an adaptive weighting function $\beta(\tau_i^t) \in [0, 1]$, which controls the reliance on the knowledge-distilled signal according to the degree of staleness. The aggregation step in Algorithm 1 (line 6) becomes:

$$\begin{aligned} \Delta_i^{\text{KD}} &\leftarrow \text{KD-REVIVE}(\tilde{\mathbf{x}}_i^{(t-\tau_i^t)}, \mathbf{x}^{(t)}), \\ \mathbf{x}^{(t+1)} &\leftarrow \mathbf{x}^{(t)} + \eta_s [(1 - \beta(\tau_i^t))\Delta_i^{(t-\tau_i^t)} + \beta(\tau_i^t)\Delta_i^{\text{KD}}] \end{aligned} \quad (4)$$

where $\text{KD-REVIVE}(\cdot)$ encapsulates our proposed DFKD mechanism. The function $\beta(\tau_i^t) \in [0, 1]$ is a non-decreasing mapping of the staleness τ_i^t , such that the server increasingly trusts the knowledge-based update as the incoming update becomes more outdated. Intuitively, when $\tau_i^t \approx 0$, the client model is nearly synchronized, and the raw parameter update remains reliable, so $\beta(\tau_i^t) \approx 0$; conversely, when τ_i^t is large, $\beta(\tau_i^t) \approx 1$, letting the server rely more on the distilled knowledge extracted from the stale client model. The specific choice of $\beta(\tau_i^t)$ and its empirical evaluation are detailed in Section 4.

Challenges of integrating KD in AFL. While incorporating KD into AFL offers a promising path to mitigating staleness, it introduces several unique challenges arising from the lack of shared data, dynamic teacher models, and non-IID client distributions. We summarize three key challenges and our solutions as follows:

(a) *Lack of distillation data.* In standard KD practice, a public or server-accessible dataset is required to mediate the knowledge transfer between the teacher and the student models. However, in FL, such data is rarely available due to privacy and communication constraints. Unlike some of the prior KD-based FL methods assuming available public data (Itahara et al., 2021; Fan et al., 2024; Qin et al., 2024), our method performs *DFKD*. The proposed KD-REVIVE module generates synthetic pseudo-data using both the client’s updated model and the server model, enabling distillation entirely without access to real data.

(b) *Dynamic teachers and need for lightweight operations.* In classical KD or DFKD setups, the teacher model is typically a fixed, fully trained oracle. In FL, however, client models continually evolve and arrive as partially trained teachers. Synthesizing transferable knowledge from such transient teachers is non-trivial. Moreover, the distillation process must remain computationally light to avoid turning the server into a bottleneck. To address these issues, we adopt a lightweight meta-learning strategy inspired by (Fang et al., 2022), maintaining a single generator that evolves throughout training. This generator efficiently adapts at each round to the incoming client models and adds produced synthetic samples into a synthetic KD dataset (\mathcal{D}_{KD}) which is initially empty in the beginning of the training.

(c) *Data heterogeneity across clients.* Due to limited data size and non-IID distributions, each client’s up-

date tends to overfit to its local data. Consequently, using a single client as a teacher can lead to biased or inconsistent knowledge transfer. To mitigate this, we introduce *multi-teacher distillation*. The server maintains a KD buffer \mathcal{C} of size c that stores the most recent client models. During distillation, we leverage all buffered teachers jointly for a more balanced and representative signal for generator training and distillation. To better exploit client-specific information, we assume the server has access to (or can estimate) the empirical label distributions of clients’ local datasets, a practical assumption adopted in prior FL work (Luo and Wu, 2021; Zec et al., 2025; Xu et al., 2025; Li et al., 2021; Ruan et al., 2024). Methods for label-distribution estimation exist but are beyond the scope of this paper (Ramakrishna and Dán, 2022; Duan et al., 2023).

By addressing these challenges, FEDREVIVE efficiently transfers informative knowledge from stale updates while preserving data privacy and scalability, as detailed next.

3.2 Detailed Steps of KD-Revive

When the server receives an updated model $\tilde{\mathbf{x}}_i^{(t-\tau_i^t)}$ from client i (Algorithm 1, line 4), it executes the KD-REVIVE procedure mentioned in eq. (4) to compute a data-free knowledge-distilled update. This procedure consists of four main steps: (1) updating the model buffer, (2) generator training and synthesizing samples, (3) meta-update of the generator, and (4) multi-teacher distillation. We detail these steps below.

(1) Update the model buffer. The server maintains a KD buffer \mathcal{C} of size c , which stores the most recently received client models for use as teacher models in the subsequent distillation process. Upon receiving a new model $\tilde{\mathbf{x}}_i^{(t-\tau_i^t)}$, the buffer is updated as:

$$\mathcal{C} \leftarrow \mathcal{C} - \{\text{oldest model in } \mathcal{C}\} + \{\tilde{\mathbf{x}}_i^{(t-\tau_i^t)}\}.$$

Initially, \mathcal{C} is empty and accumulates models until reaching size c , after which the oldest entry is removed each time a new client model arrives. This rolling buffer ensures that the distillation process leverages the most recent and diverse set of client knowledge.

(2) Generator training. A generator G_θ parameterized by θ is initialized once at the start of training. We employ a meta-learning strategy inspired by (Fang et al., 2022) to enable the generator to evolve continually with the incoming client models. At each KD-REVIVE step, we initialize a batch of latent random vectors \mathbf{z} and corresponding target labels \mathbf{y}_z , assigned uniformly across all classes. Over K_{KD} synthesis iterations, the generator parameters θ' (initialized as $\theta' \leftarrow \theta$) and latent variables \mathbf{z} are jointly optimized to

minimize the synthesis loss $\mathcal{L}_{\text{synth}}$, using the learning rate η_{synth} :

$$(\mathbf{z}, \boldsymbol{\theta}') \leftarrow (\mathbf{z}, \boldsymbol{\theta}') - \eta_{\text{synth}} \nabla_{(\mathbf{z}, \boldsymbol{\theta}')} \mathcal{L}_{\text{synth}}(G_{\boldsymbol{\theta}'}(\mathbf{z})).$$

The synthesis loss $\mathcal{L}_{\text{synth}}$, defined as:

$$\mathcal{L}_{\text{synth}} = \alpha_{\text{target}} \mathcal{L}_{\text{target}} + \alpha_{\text{feature}} \mathcal{L}_{\text{feature}} + \alpha_{\text{adv}} \mathcal{L}_{\text{adv}}, \quad (5)$$

is designed to produce informative pseudo-samples for the teachers and consists of weighted sum of three components:

- **Target Loss ($\mathcal{L}_{\text{target}}$):** Encourages the teacher predictions on $G_{\boldsymbol{\theta}'}(\mathbf{z})$ to align with the assigned target labels $\mathbf{y}_{\mathbf{z}}$.
- **Feature Loss ($\mathcal{L}_{\text{feature}}$):** Matches the intermediate feature statistics of the teacher on the generated input to those of running statistics of the model from client local training.
- **Adversarial Loss (\mathcal{L}_{adv}):** For inputs where the student and teacher already agree, penalizes the match of other logits to amplify the informative discrepancy and strengthen the distillation signal.

All models in \mathcal{C} are used to compute $\mathcal{L}_{\text{synth}}$, where for each synthetic sample in the batch, the teachers’ individual losses are combined by a weighted average, with each teacher’s weight corresponding to its client’s proportion of the target label assigned to that sample. After K_{KD} updates, the synthetic sample of optimized pair $(\mathbf{z}^*, \boldsymbol{\theta}^*)$ that yields the lowest $\mathcal{L}_{\text{synth}}$ and their corresponding target labels are added to the synthetic dataset:

$$\mathcal{D}_{\text{KD}} \leftarrow \mathcal{D}_{\text{KD}} \cup \{(G_{\boldsymbol{\theta}^*}(\mathbf{z}^*), \mathbf{y}_{\mathbf{z}^*})\}.$$

\mathcal{D}_{KD} is bounded to a fixed capacity to discard the oldest samples once the limit is reached.

(3) Meta-update of the generator. After synthesizing informative pseudo-samples, we perform a meta-update to refine the generator parameters $\boldsymbol{\theta}$. Following (Fang et al., 2022), we employ a Reptile-like meta-learning (Nichol et al., 2018) update to stabilize our training under evolving teacher models. The meta-update interpolates between the optimized parameters $\boldsymbol{\theta}'$ (final parameters after synthesis loop) and the previous meta-parameters $\boldsymbol{\theta}$:

$$\boldsymbol{\theta} \leftarrow (1 - \lambda) \boldsymbol{\theta}' + \lambda \boldsymbol{\theta}.$$

This update ensures that $G_{\boldsymbol{\theta}}$ gradually adapts to the changing set of teacher models without catastrophic drift, allowing the generator to retain generalizable

knowledge while continuously evolving throughout the federated training process. Meta-learning thus prevents divergence and maintains stability in generating synthetic data across asynchronous, dynamic updates.

(4) Multi-teacher distillation. Finally, the synthetic dataset \mathcal{D}_{KD} is used to distill knowledge from the teacher models in the KD buffer \mathcal{C} into the student model \mathbf{x}_s , which is initialized as the current server model, $\mathbf{x}_s \leftarrow \mathbf{x}^t$. For K_{KD} distillation steps, the student model is updated to minimize the Kullback–Leibler (KL) divergence between the logits of each teacher $\mathbf{x}_i \in \mathcal{C}$ and the student model, averaged across all buffered teachers:

$$\mathbf{x}_s \leftarrow \mathbf{x}_s - \eta_{\text{KD}} \frac{1}{|\mathcal{C}|} \sum_{\mathbf{x}_i \in \mathcal{C}} \left[\nabla_{\mathbf{x}_s} \text{KL}(\mathbf{x}_i(\mathbf{u}_i) \parallel \mathbf{x}_s(\mathbf{u}_i)) \right],$$

where $\mathbf{u}_i \in \mathcal{D}_{\text{KD}}$ denotes an input batch sampled from \mathcal{D}_{KD} according to the label distribution associated with the client that produced Δ_i . This multi-teacher setting allows the server to aggregate and align knowledge from multiple clients simultaneously, reducing the effect of heterogeneity across clients. Finally, the KD update is computed as:

$$\Delta_{\text{KD}}^t = \mathbf{x}_s - \mathbf{x}^t,$$

and used in the hybrid aggregation rule.

3.3 Overhead Analysis

FEDREVIVE introduces additional computation on the central server due to the generator training and multi-teacher distillation before hybrid aggregation. However, this overhead is minimal and does not compromise the scalability of AFL. The KD process mainly involves lightweight stochastic gradient updates, and our experiments show effective results with only $K_{\text{KD}}=2$ and $K_{\text{KD}}=10$. Given the high computational capacity of central servers, these computations are negligible compared to the dominant cost of network communication latency and local training (Lai et al., 2021), and FEDREVIVE has the same communication overhead as FedAvg. Consequently, DFKD adds little to the overall training time while substantially improving stability and convergence by leveraging stale updates more effectively. Also, FEDREVIVE has the same memory overhead as FedAvg as discussed in Appendix C.

4 Experiments and Results

We evaluate our proposed method and baselines on both image classification and text classification tasks under diverse system conditions. In all experiments, we assume a large-scale FL environment consisting of 1000 clients, where only 10% are active at any given

time, selected uniformly at random, which reflects the intermittent availability of edge devices like mobile phones. To induce data heterogeneity, we follow the common Dirichlet partitioning scheme with different α values following (Acar et al., 2021), unless the dataset is naturally partitioned. In the main text, we present the results with high data heterogeneity, Dirichlet parameter $\alpha=0.5$, and refer the reader to the Appendix A for the results with milder heterogeneity ($\alpha=1$) and IID distribution.

Since our focus is on AFL, all results are presented with respect to simulated wall-clock time, which accounts for realistic computation and communication delays. To emulate system heterogeneity, we categorize clients into *slow*, *medium*, and *fast* groups according to their computation and communication speeds. Each client is assigned random delay parameters based on its group. When a client participates in a training round, its local computation and upload durations are sampled from its random parameters, ensuring stochastic time variations across rounds. This setup results in both system heterogeneity across clients and rounds, reflecting real environments. We plot the distribution of update staleness in server rounds from a sample experiment for a fully asynchronous algorithm (no update buffer) in Figure 1. It is shown in the figure that the staleness distribution is long-tailed due to slow clients. The figure further validates the simulation’s alignment with real practice, matching the staleness distribution observed in real-world experiments with millions of clients (Nguyen et al., 2022).

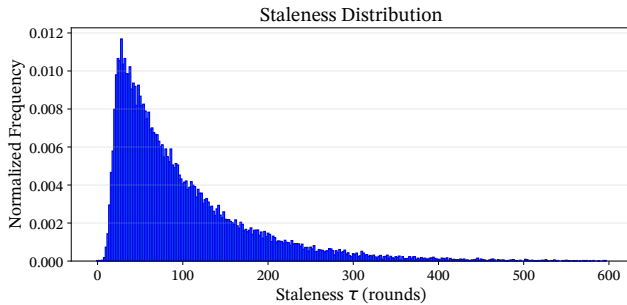


Figure 1: Distribution of update staleness across server rounds for a fully asynchronous setup. The distribution aligns with real-world AFL systems reported in (Nguyen et al., 2022).

All reported results are averaged over three random seeds, with shaded regions indicating the standard error. For every compared method, we tune hyperparameters on validation performance. Since asynchronous algorithms tend to exhibit fluctuating behavior, where model performance can slightly and temporarily degrade, we report the *best-so-far* test performance over

time for clearer visualization. The raw unprocessed accuracy curves are provided in Appendix B due to space limitations.

4.1 Datasets and Models

We benchmark our method on both image and text classification tasks using the following datasets and model architectures:

- **CIFAR-10:** A 10-class RGB image classification task. We employ the ResNet-18 architecture (11.2M parameters).
- **CIFAR-100:** A 100-class RGB image classification task using the same ResNet-18.
- **FEMNIST:** The Federated Extended MNIST (FEMNIST) dataset (Caldas et al., 2019) consists of a 62-class grayscale handwritten character classification task. It provides a natural user-level partition across approximately 3500 writers. We adopt a lightweight multi-layer convolutional neural network (CNN) model (421k parameters).
- **20NewsGroups:** A topic-based news text classification task. We utilize a pretrained T5-small (Raffel et al., 2023) transformer model with its embedding layer frozen during training (35.6M parameters).

Except for FEMNIST, we simulate 1000 clients by repeatedly sampling the dataset to allocate 350 samples per client. For FEMNIST, we randomly select 1000 users from the natural partition, each corresponding to an individual client.

4.2 Baselines

We compare our proposed FEDREVIVE with representative baselines from the literature. The methods used in our experiments are summarized below:

- **FedAvg:** The vanilla synchronous FL algorithm (McMahan et al., 2017), where the server waits for all active clients to complete their local updates before aggregation. The updates have no staleness by design but generally round times are large due to waiting for slow clients (i.e., *stragglers*) (Xie et al., 2019).
- **FedBuff:** The buffered asynchronous variant of FEDAVG (Nguyen et al., 2022), which extends the vanilla asynchronous FEDAVG (Xie et al., 2019) by maintaining a buffer of incoming client updates before aggregation. When the buffer size is set to 1, FEDBUFF reduces to asynchronous FEDAVG. Since tuning the buffer size yields superior performance, we report results only for FEDBUFF as the representative baseline. Eq. (3) shows the aggregation step.

- **FedRevive:** Our proposed method. In all experiments, we set $K_{KD} = 2$ and $K_{KD} = 10$ for the synthetic data generation and KD steps, respectively.

- **DD-FedRevive:** An ablation variant, Data-Driven-FEDREVIVE, where instead of the proposed meta-learned generator-based data synthesis, the server is assumed to have access to a small public dataset that approximates the average client distribution. The public dataset size is fixed to 1/6 of total train size across clients, and KD is performed directly on this data. Algorithmically, this corresponds to the KD step of FEDREVIVE without generator-based synthesis. This setting is included only for ablation purposes, as it assumes unrealistic access to public data in FL.

- **AFL-DW:** Prior asynchronous FL works (Chen et al., 2019; Shi et al., 2020; Lu et al., 2020) have proposed down-weighting stale updates to mitigate their negative effect on convergence. Although specific decay functions vary across studies, the common idea is to reduce the influence of more stale updates. To examine whether the improvement of FEDREVIVE arises primarily from integrating KD update or reducing the effect of stale updates in Eq. (4), we include AFL-Down Weighting (AFL-DW) as an ablation that applies only the down-weighting strategy without any KD synthesis or distillation. Its aggregation rule is modified from Eq. (3) to $\mathbf{x}^{(t+1)} \leftarrow \mathbf{x}^{(t)} + \eta_s(1 - \beta(\tau_i^t))\Delta_i$, while keeping all other hyperparameters and β function choice identical to those in FEDREVIVE.

4.3 Image Task Results

In CIFAR-10, CIFAR-100, and FEMNIST, for the synthesis module in our proposed FEDREVIVE, we employ the same lightweight generator architecture as in (Fang et al., 2022), which maps a latent noise vector to a 2D variable through a linear projection followed by a CNN block. Figure 2 presents the test accuracy curves of all compared methods with respect to simulated time. As observed, the synchronous baseline FEDAVG suffers from significantly long global round times since the server must wait for all selected clients to complete their local training. Although this approach avoids staleness, the overall convergence speed is limited by the slowest participants. In contrast, FEDBUFF achieves much faster convergence by allowing asynchronous updates, and its buffering mechanism mitigates the impact of excessively stale updates. Its final accuracy is consistent with previous findings in asynchronous FL literature (Askin et al., 2024). Our proposed method, FEDREVIVE, converges notably faster than FEDBUFF. Even though clients operate under the same asynchronous conditions, each update in FEDREVIVE contributes more effectively, as the model continually transfers knowledge from stale client mod-

els through the DFKD process. This enables faster and more stable learning compared to parameter space aggregation alone.

Moreover, by leveraging synthetic data generated by the evolving generator, FEDREVIVE achieves substantially higher final accuracy than all baselines. The variant DD-FEDREVIVE, which assumes access to a small public dataset for distillation, exhibits the fastest convergence due to the immediate availability of real data. However, FEDREVIVE surpasses DD-FEDREVIVE in final performance, as the fixed public dataset in DD-FEDREVIVE may lead to partial overfitting, while the synthetic data in FEDREVIVE adaptively evolves alongside the training, yielding richer and more diverse knowledge transfer. Finally, the performance of AFL-DW remains considerably lower than that of FEDREVIVE, confirming that the improvement of our method arises not primarily from down-weighting stale updates but from the proposed DFKD mechanism itself.

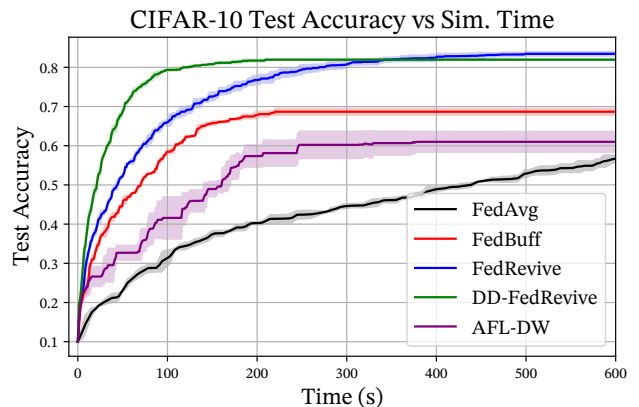


Figure 2: CIFAR-10 test accuracy over simulated time. FEDREVIVE converges faster and attains higher final accuracy than baseline FEDBUFF (0.83 ± 0.01 vs 0.69 ± 0.01).

We provide the test accuracy curves over simulated training time for CIFAR-100 in Figure 3. Compared to CIFAR-10, the CIFAR-100 task involves 100 classes, which significantly increases the difficulty of class-conditioned data generation and KD. This makes it a more challenging benchmark for evaluating the robustness of data-free distillation. Once the client models (serving as teachers in our DFKD framework) reach reasonable accuracy, we observe that FEDREVIVE begins to outperform the asynchronous baseline FEDBUFF. The performance gap between DD-FEDREVIVE and other methods widens in this more complex task, as the presence of a public dataset at the server side provides a larger relative advantage when class diversity increases. Nevertheless, in terms of final accuracy, we observe the

same trend as in CIFAR-10 where both FEDREVIVE and DD-FEDREVIVE yield substantial improvements over the baselines.

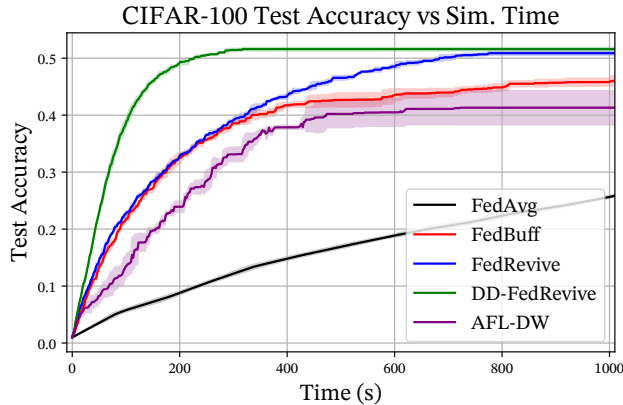


Figure 3: CIFAR-100 test accuracy vs simulated time. The performance gap between FEDREVIVE (final accuracy: 0.51 ± 0.01) and FEDBUFF (final accuracy: 0.46 ± 0.01) widens when the client models are trained enough to show sufficient teacher performance in this harder 100-class task.

Figure 4 shows the test accuracy curves for the FEMNIST dataset. In this task, the adverse effect of stale updates appears to be less pronounced than in the CIFAR-10 and CIFAR-100 experiments. This is likely due to the relatively simpler visual patterns of handwritten digits and characters, which make the feature space easier to learn. Consequently, the asynchronous methods perform more closely to one another, while our DFKD-augmented FEDREVIVE still surpasses all baselines and achieves the highest final accuracy.

4.4 Text Task Results

For the text domain task, 20NewsGroups, we use the encoder-only T5-small architecture with an additional classification head consisting of linear layers. The head operates on the final hidden state of the first token after the transformer layers, producing the class logits. For each sample, we prepend a dummy token at the first position and limit the sequence length to 128 tokens. For this experiment, we modify our synthetic data generation process to better accommodate the properties of text data. Unlike images, text data lies in a discrete and highly structured space, and prior data-free distillation works in NLP typically rely on external or generated corpora (Palo et al., 2024; Xu et al., 2024; Tian et al., 2025). In our method, instead of employing a generator network, we meta-learn a set of four soft prompt vectors inserted immediately after the dummy prediction token, following recent soft

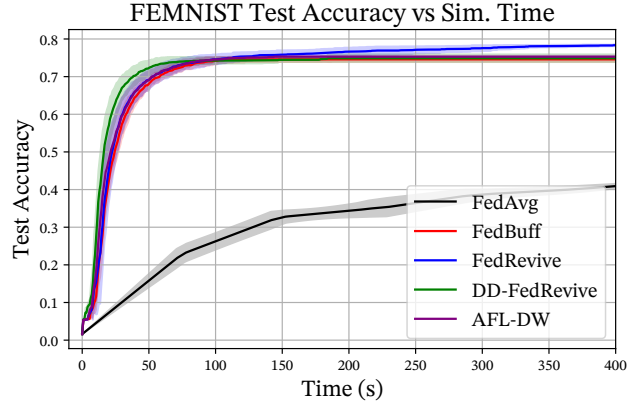


Figure 4: FEMNIST accuracy curves. Although the task is simpler than CIFAR-10 and CIFAR-100, leading to similar convergence rates from all asynchronous baselines, FEDREVIVE (final accuracy: 0.78 ± 0.00) still has faster convergence than FEDBUFF (final accuracy: 0.75 ± 0.01).

prompt learning works (Lester et al., 2021; Gu et al., 2022).

To initialize the remaining prompt embeddings, we utilize synthetic sentences generated by a small instruction-tuned language model (Zhang et al., 2024) with approximately 1B parameters. For each class label, we prompt the model to generate a short random news snippet about the corresponding topic. To ensure that these generated samples do not leak meaningful information or overly align with the downstream task, we use a high sampling temperature and a small capability model for generation. As shown in Section 4.5, this generated data performs poorly on the actual task, confirming that it only serves as a weak linguistic prior for initializing the embedding vectors in our DFKD process. In this configuration, the generator parameters θ correspond to the four meta-learned soft prompt vectors, while the latent variable \mathbf{z} denotes the remaining embedding vectors initialized with class-conditioned synthetic text outputs.

Figure 5 shows the test accuracy curves for the 20NewsGroups task over simulated training time. The proposed FEDREVIVE consistently outperforms all baselines. In this setting, AFL-DW performs comparably to FEDBUFF. Among all methods, FEDREVIVE and its data-driven variant DD-FEDREVIVE achieve the fastest convergence.

Overall Convergence Speed. Table 1 summarizes the mean simulated time required by each method to reach 85% of the best FEDBUFF accuracy across all benchmarks. Consistent with the curve analyses above,

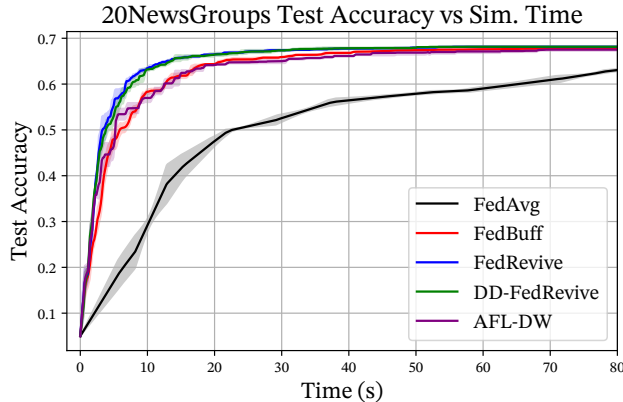


Figure 5: 20NewsGroups test accuracy curves. FEDREVIVE and FEDBUFF reach the same final accuracy (0.68), with FEDREVIVE surpassing the baseline in convergence speed.

FEDREVIVE achieves remarkably faster convergence than the asynchronous baseline FEDBUFF, demonstrating up to 21.0% shorter time-to-target on average, confirming that integrating DFKD substantially improves the efficiency of asynchronous training without requiring public data. The variant DD-FEDREVIVE, which assumes access to a small public dataset, attains the fastest convergence overall but remains only a hypothetical upper bound due to its unrealistic assumption of data availability.

4.5 Synthetic Text Data Ablation

For the text task, one may question the effect of using language model-generated data for initializing \mathbf{z} in the synthesis step of FEDREVIVE. To evaluate its impact, we perform centralized training using only the generated synthetic data and test on the actual dataset, 20NewsGroups. The resulting best test accuracy is $48.08\% \pm 0.22\%$, which is considerably lower than the federated results achieved by any of the compared methods in Figure 5. This confirms that the generated samples are not suitable for the actual task but serve effectively as a neutral initialization of language priors, enabling stable and efficient synthetic data generation within our DFKD process.

4.6 Hyperparameters and β Function Selection

For each compared method, we tune hyperparameters individually on respective tasks. For our proposed FEDREVIVE, we use the same generator configuration across all vision tasks, as it consistently yields strong performance.

Table 1: Mean \pm std simulated time (in seconds) to reach 85% of best FEDBUFF accuracy across datasets. Lower values indicate faster convergence; FEDREVIVE consistently achieves shorter time-to-target than FEDBUFF.

Method	CIFAR-10	CIFAR-100
FEDAVG	628.6 ± 30.0	>1000
FEDBUFF	96.4 ± 2.0	318.9 ± 20.4
AFL-DW	184.7 ± 0.9	451.5 ± 21.5
FEDREVIVE	65.5 ± 1.5	304.6 ± 12.4
DD-FEDREVIVE	28.6 ± 1.1	101.6 ± 5.4

Method	20NewsGroups	FEMNIST
FEDAVG	53.4 ± 1.5	>1000
FEDBUFF	9.9 ± 0.5	38.2 ± 4.5
AFL-DW	10.8 ± 1.3	35.3 ± 6.2
FEDREVIVE	6.1 ± 0.8	34.7 ± 6.6
DD-FEDREVIVE	6.2 ± 0.7	25.4 ± 5.0

The choice of the weighting function β is particularly important, as it controls the balance between the parameter-space update and the KD update in Eq. (4). Intuitively, when the received client update has low staleness, the server should rely more on the original parameter-space update, whereas for highly stale updates, the KD component should be emphasized. To study the effect of different β formulations, we experiment with multiple functional families on the CIFAR-10 task and analyze their impact on convergence and stability. Figure 6 illustrates several candidate β functions with distinct growth behaviors. After comparing their performance, we select the 1-cosine schedule, which provides a smooth, monotonic transition from parameter-space to KD-dominated aggregation and involves only a single tunable parameter controlling the transition rate. The function remains constant once it first reaches 1. Detailed descriptions of all hyperparameter values are provided in Appendix D to ensure full reproducibility of our results.

5 Conclusion

Asynchronous federated learning algorithms offer the scalability required for large-scale decentralized training and cross-device FL, yet suffer from the staleness of delayed updates. Although stale updates can hinder convergence, they still contain valuable information about the clients’ local data. In this work, we introduced FEDREVIVE, a scalable asynchronous FL framework that extracts and transfers this information through data-free knowledge distillation. By combining lightweight meta-learned synthetic data generation with multi-teacher distillation, our approach effectively mitigates staleness while preserving data privacy and system efficiency. Extensive experiments on vision

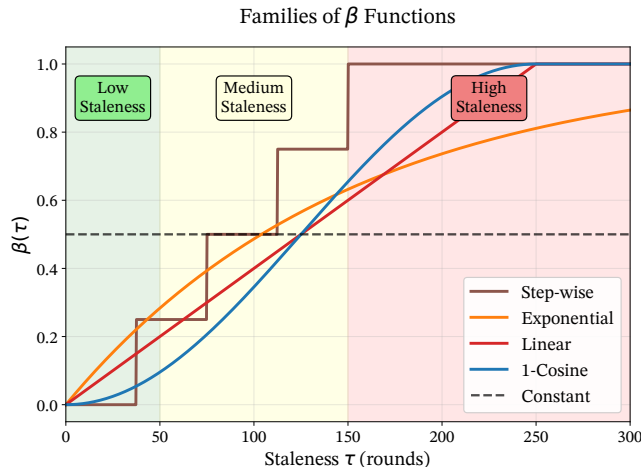


Figure 6: Different candidate β scheduling functions controlling the mix between parameter aggregation and DFKD updates. 1-cosine schedule is chosen, as it empirically shows the best performance on the CIFAR-10 task.

and text tasks demonstrate that FEDREVIVE substantially improves convergence speed and final accuracy compared to existing asynchronous baselines. Looking ahead, extending our framework with pretrained generative models for applicable data modalities presents a promising direction, as high-quality public generative models continue to advance.

Acknowledgements

This work was partially supported by the US National Science Foundation under grants CNS-2106891 and CNS-2409138 to CJW and CCF 2045694, CNS-2112471, CPS-2111751, and ONR N00014-23-1-2149 to G.J.

References

- Acar, D. A. E., Zhao, Y., Matas, R., Mattina, M., Whatmough, P., and Saligrama, V. (2021). Federated learning based on dynamic regularization. In *International Conference on Learning Representations*.
- Askin, B., Sharma, P., Joe-Wong, C., and Joshi, G. (2024). Fedast: federated asynchronous simultaneous training. In *Proceedings of the Fortieth Conference on Uncertainty in Artificial Intelligence, UAI '24*. JMLR.org.
- Bonawitz, K. A., Eichner, H., Grieskamp, W., Huba, D., Ingerman, A., Ivanov, V., Kiddon, C., Konečný, J., Mazzocchi, S., McMahan, H. B., Overveldt, T. V., Petrou, D., Ramage, D., and Roselander, J. (2019). Towards federated learning at scale: System design. *CoRR*, abs/1902.01046.
- Caldas, S., Duodu, S. M. K., Wu, P., Li, T., Konečný, J., McMahan, H. B., Smith, V., and Talwalkar, A. (2019). Leaf: A benchmark for federated settings.
- Chen, M., Mao, B., and Ma, T. (2021). Fedsta: A staleness-aware asynchronous federated learning algorithm with non-iid data. *Future Generation Computer Systems*, 120:1–12.
- Chen, Y., Ning, Y., Slawski, M., and Rangwala, H. (2020). Asynchronous Online Federated Learning for Edge Devices with Non-IID Data. In *2020 IEEE International Conference on Big Data (Big Data)*, pages 15–24, Los Alamitos, CA, USA. IEEE Computer Society.
- Chen, Y., Sun, X., and Jin, Y. (2019). Communication-efficient federated deep learning with layerwise asynchronous model update and temporally weighted aggregation. *IEEE transactions on neural networks and learning systems*, 31(10):4229–4238.
- Cui, H., Cipar, J., Ho, Q., Kim, J. K., Lee, S., Kumar, A., Wei, J., Dai, W., Ganger, G. R., Gibbons, P. B., et al. (2014). Exploiting bounded staleness to speed up big data analytics. In *USENIX Annual Technical Conference (ATC)*, pages 37–48.
- Dean, J. et al. (2012). Large scale distributed deep networks. In *Advances in Neural Information Processing Systems*, pages 1223–1231.
- Duan, J.-H., Li, W., Zou, D., Li, R., and Lu, S. (2023). Federated learning with data-agnostic distribution fusion. In *2023 IEEE/CVF Conference on Computer Vision and Pattern Recognition (CVPR)*, pages 8074–8083.
- Dutta, S., Joshi, G., Ghosh, S., Dube, P., and Nagpurkar, P. (2018). Slow and Stale Gradients Can Win the Race: Error-Runtime Trade-offs in Distributed SGD. *Proceedings of the International Conference on Artificial Intelligence and Statistics (AISTATS)*.
- Fan, B., Jiang, S., Su, X., Tarkoma, S., and Hui, P. (2024). A Survey on Model-heterogeneous Federated Learning: Problems, Methods, and Prospects. In *2024 IEEE International Conference on Big Data (BigData)*, pages 7725–7734, Los Alamitos, CA, USA. IEEE Computer Society.
- Fang, G., Mo, K., Wang, X., Song, J., Bei, S., Zhang, H., and Song, M. (2022). Up to 100x faster data-free knowledge distillation. *Proceedings of the AAAI Conference on Artificial Intelligence*, 36(6):6597–6604.
- Gao, L., Zhang, Z., and Wu, C. (2025). Feddtg: federated data-free knowledge distillation via three-player generative adversarial networks.
- Gu, Y., Han, X., Liu, Z., and Huang, M. (2022). PPT: Pre-trained prompt tuning for few-shot learning. In

- Muresan, S., Nakov, P., and Villavicencio, A., editors, *Proceedings of the 60th Annual Meeting of the Association for Computational Linguistics (Volume 1: Long Papers)*, pages 8410–8423, Dublin, Ireland. Association for Computational Linguistics.
- Gupta, S., Zhang, W., and Wang, F. (2016). Model accuracy and runtime tradeoff in distributed deep learning: A systematic study. In *International Conference on Data Mining*, pages 171–180.
- Hinton, G. E., Vinyals, O., and Dean, J. (2015). Distilling the knowledge in a neural network. *CoRR*, abs/1503.02531.
- Ho, Q., Cipar, J., Cui, H., Lee, S., Kim, J. K., Gibbons, P. B., Gibson, G. A., Ganger, G., and Xing, E. P. (2013). More effective distributed ml via a stale synchronous parallel parameter server. In *Advances in Neural Information Processing Systems*, pages 1223–1231.
- Itahara, S., Nishio, T., Koda, Y., Morikura, M., and Yamamoto, K. (2021). Distillation-based semi-supervised federated learning for communication-efficient collaborative training with non-iid private data. *IEEE Transactions on Mobile Computing*, 22(1):191–205.
- Jiao, X., Yin, Y., Shang, L., Jiang, X., Chen, X., Li, L., Wang, F., and Liu, Q. (2020). TinyBERT: Distilling BERT for natural language understanding. In Cohn, T., He, Y., and Liu, Y., editors, *Findings of the Association for Computational Linguistics: EMNLP 2020*, pages 4163–4174, Online. Association for Computational Linguistics.
- Koloskova, A., Stich, S. U., and Jaggi, M. (2022). Sharper convergence guarantees for asynchronous sgd for distributed and federated learning. *Advances in Neural Information Processing Systems*, 35:17202–17215.
- Lai, F., Dai, Y., Zhu, X., Madhyastha, H. V., and Chowdhury, M. (2021). FedScale: Benchmarking model and system performance of federated learning. In *Proceedings of the First Workshop on Systems Challenges in Reliable and Secure Federated Learning, ResilientFL '21*, page 1–3, New York, NY, USA. Association for Computing Machinery.
- Lee, S., Yoo, K., and Kwak, N. (2020). Edge bias in federated learning and its solution by buffered knowledge distillation. *arXiv preprint arXiv:2010.10338*.
- Lester, B., Al-Rfou, R., and Constant, N. (2021). The power of scale for parameter-efficient prompt tuning. In Moens, M.-F., Huang, X., Specia, L., and Yih, S. W.-t., editors, *Proceedings of the 2021 Conference on Empirical Methods in Natural Language Processing*, pages 3045–3059, Online and Punta Cana, Dominican Republic. Association for Computational Linguistics.
- Li, A., Zhang, L., Tan, J., Qin, Y., Wang, J., and Li, X.-Y. (2021). Sample-level data selection for federated learning. In *IEEE INFOCOM 2021-IEEE Conference on Computer Communications*, pages 1–10. IEEE.
- Li, D. and Wang, J. (2019). Fedmd: Heterogenous federated learning via model distillation.
- Li, L., Gou, J., Yu, B., Du, L., and Tao, Z. Y. D. (2024). Federated distillation: A survey. *arXiv preprint arXiv:2404.08564*.
- Lian, X., Huang, Y., Li, Y., and Liu, J. (2015). Asynchronous parallel stochastic gradient for nonconvex optimization. In *Advances in Neural Information Processing Systems*, pages 2737–2745.
- Lin, T., Kong, L., Stich, S. U., and Jaggi, M. (2020). Ensemble distillation for robust model fusion in federated learning. *Advances in neural information processing systems*, 33:2351–2363.
- Lopes, R. G., Fenu, S., and Starner, T. (2017a). Data-free knowledge distillation for deep neural networks.
- Lopes, R. G., Fenu, S., and Starner, T. (2017b). Data-free knowledge distillation for deep neural networks.
- Lu, C., Sun, Y., Li, P., and Yang, Z. (2025). Corrected with the latest version: Make robust asynchronous federated learning possible.
- Lu, X., Liao, Y., Lio, P., and Hui, P. (2020). Privacy-preserving asynchronous federated learning mechanism for edge network computing. *IEEE Access*, 8:48970–48981.
- Luo, B., Xiao, W., Wang, S., Huang, J., and Tassioulas, L. (2022). Tackling system and statistical heterogeneity for federated learning with adaptive client sampling. In *IEEE INFOCOM 2022 - IEEE Conference on Computer Communications*, page 1739–1748. IEEE Press.
- Luo, J. and Wu, S. (2021). FedSld: Federated learning with shared label distribution for medical image classification.
- Mansourian, A. M., Ahmadi, R., Ghafouri, M., Babaei, A. M., Golezani, E. B., yasamani ghamchi, Z., Ramezani, V., Taherian, A., Dinashi, K., Miri, A., and Kasaei, S. (2025). A comprehensive survey on knowledge distillation. *Transactions on Machine Learning Research*.
- McMahan, B., Moore, E., Ramage, D., Hampson, S., and Arcas, B. A. y. (2017). Communication-Efficient Learning of Deep Networks from Decentralized Data. In Singh, A. and Zhu, J., editors, *Proceedings of the*

- 20th International Conference on Artificial Intelligence and Statistics, volume 54 of *Proceedings of Machine Learning Research*, pages 1273–1282. PMLR.
- Mitliagkas, I., Zhang, C., Hadjis, S., and Ré, C. (2016). Asynchrony begets momentum, with an application to deep learning. In *Allerton Conference on Communication, Control, and Computing*, pages 997–1004. IEEE.
- Nguyen, J., Malik, K., Zhan, H., Yousefpour, A., Rabbat, M., Malek, M., and Huba, D. (2022). Federated learning with buffered asynchronous aggregation. In Camps-Valls, G., Ruiz, F. J. R., and Valera, I., editors, *Proceedings of The 25th International Conference on Artificial Intelligence and Statistics*, volume 151 of *Proceedings of Machine Learning Research*, pages 3581–3607. PMLR.
- Nichol, A., Achiam, J., and Schulman, J. (2018). On first-order meta-learning algorithms. *arXiv preprint arXiv:1803.02999*.
- Palo, F. D., Singhi, P., and Fadlallah, B. H. (2024). Performance-guided LLM knowledge distillation for efficient text classification at scale. In Al-Onaizan, Y., Bansal, M., and Chen, Y.-N., editors, *Proceedings of the 2024 Conference on Empirical Methods in Natural Language Processing*, pages 3675–3687, Miami, Florida, USA. Association for Computational Linguistics.
- Qin, L., Zhu, T., Zhou, W., and Yu, P. S. (2024). Knowledge distillation in federated learning: a survey on long lasting challenges and new solutions.
- Raffel, C., Shazeer, N., Roberts, A., Lee, K., Narang, S., Matena, M., Zhou, Y., Li, W., and Liu, P. J. (2023). Exploring the limits of transfer learning with a unified text-to-text transformer.
- Ramakrishna, R. and Dán, G. (2022). Inferring class-label distribution in federated learning. In *Proceedings of the 15th ACM Workshop on Artificial Intelligence and Security*, AISC’22, page 45–56, New York, NY, USA. Association for Computing Machinery.
- Richtarik, P. (2025). Handling device heterogeneity in federated learning: The first optimal parallel sgd in the presence of data, compute and communication heterogeneity. In *Proceedings of the International Workshop on Secure and Efficient Federated Learning*, pages 1–1.
- Rieke, N., Hancox, J., Li, W., Milletari, F., Roth, H. R., Albarqouni, S., Bakas, S., Galtier, M. N., Landman, B. A., Maier-Hein, K., et al. (2020). The future of digital health with federated learning. *NPJ digital medicine*, 3(1):119.
- Ruan, Y., Zhang, X., and Joe-Wong, C. (2024). How valuable is your data? optimizing client recruitment in federated learning. *IEEE/ACM Transactions on Networking*.
- Shang, E., Liu, H., Yang, Z., Du, J., and Ge, Y. (2023). Fedbikd: Federated bidirectional knowledge distillation for distracted driving detection. *IEEE Internet of Things Journal*, 10(13):11643–11654.
- Shi, G., Li, L., Wang, J., Chen, W., Ye, K., and Xu, C. (2020). Hysync: Hybrid federated learning with effective synchronization. In *2020 IEEE 22nd International Conference on High Performance Computing and Communications; IEEE 18th International Conference on Smart City; IEEE 6th International Conference on Data Science and Systems (HPCC/SmartCity/DSS)*, pages 628–633.
- Tian, Y., Han, Y., Chen, X., Wang, W., and Chawla, N. V. (2025). Beyond answers: Transferring reasoning capabilities to smaller llms using multi-teacher knowledge distillation. In *Proceedings of the Eighteenth ACM International Conference on Web Search and Data Mining*, WSDM ’25, page 251–260, New York, NY, USA. Association for Computing Machinery.
- Wang, J., Liu, Q., Liang, H., Joshi, G., and Poor, H. V. (2020). Tackling the objective inconsistency problem in heterogeneous federated optimization. *Advances in neural information processing systems*, 33:7611–7623.
- Xie, C., Koyejo, S., and Gupta, I. (2019). Asynchronous federated optimization. *arXiv preprint arXiv:1903.03934*.
- Xu, C., Qu, Y., Xiang, Y., and Gao, L. (2023). Asynchronous federated learning on heterogeneous devices: A survey. *Computer Science Review*, 50:100595.
- Xu, K., Feng, Y., Li, J., Qi, Y., and Zhou, J. (2025). C²prompt: Class-aware client knowledge interaction for federated continual learning.
- Xu, X., Li, M., Tao, C., Shen, T., Cheng, R., Li, J., Xu, C., Tao, D., and Zhou, T. (2024). A survey on knowledge distillation of large language models.
- Yang, Q., Liu, Y., Chen, T., and Tong, Y. (2019). Federated machine learning: Concept and applications. *ACM Transactions on Intelligent Systems and Technology (TIST)*, 10(2):1–19.
- Yu, X., Cherkasova, L., Vardhan, H., Zhao, Q., Ekaireb, E., Zhang, X., Mazumdar, A., and Rosing, T. (2023). Async-hfl: Efficient and robust asynchronous federated learning in hierarchical iot networks. In *Proceedings of the 8th ACM/IEEE Conference on Internet of Things Design and Implementation*, pages 236–248.
- Zagoruyko, S. and Komodakis, N. (2017). Paying more attention to attention: Improving the performance of convolutional neural networks via attention transfer. In *International Conference on Learning Representations*.

- Zec, E. L., Breitholtz, A., and Johansson, F. D. (2025). Overcoming label shift with target-aware federated learning.
- Zhang, L., Shen, L., Ding, L., Tao, D., and Duan, L.-Y. (2022). Fine-tuning global model via data-free knowledge distillation for non-iid federated learning. In *Proceedings of the IEEE/CVF conference on computer vision and pattern recognition*, pages 10174–10183.
- Zhang, P., Zeng, G., Wang, T., and Lu, W. (2024). Tinyllama: An open-source small language model.
- Zhang, W., Gupta, S., Lian, X., and Liu, J. (2016). Staleness-aware async-sgd for distributed deep learning. In *International Joint Conference on Artificial Intelligence*, pages 2350–2356. AAAI Press.
- Zhu, Z., Hong, J., and Zhou, J. (2021). Data-free knowledge distillation for heterogeneous federated learning. In *International conference on machine learning*, pages 12878–12889. PMLR.

Appendix

A Results with Different Heterogeneity Levels

We provide additional experimental results under different levels of data heterogeneity. For the CIFAR-10, CIFAR-100, and 20NewsGroups datasets, we show the test accuracy curves when client data is distributed with milder non-IID partition ($\alpha = 1$) and with fully homogeneous (IID) distribution. See Figures 7–12 for the results. Note that the FEMNIST dataset is naturally partitioned by real users and thus does not allow controlling its heterogeneity. Hence, it is excluded from this analysis.

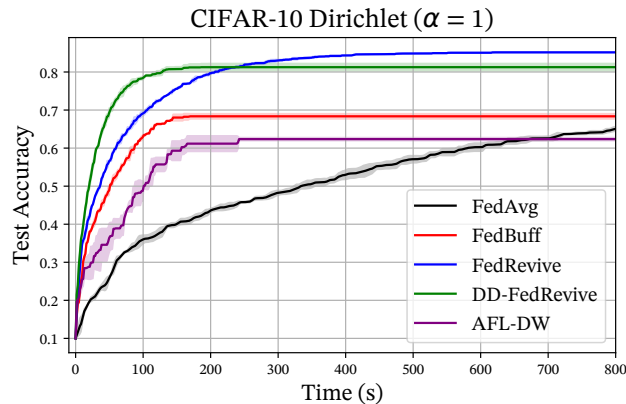


Figure 7: CIFAR-10 test accuracy over simulated time under milder heterogeneity ($\alpha = 1$). FEDREVIVE converges faster and achieves higher final accuracy than the baseline FEDBUFF.

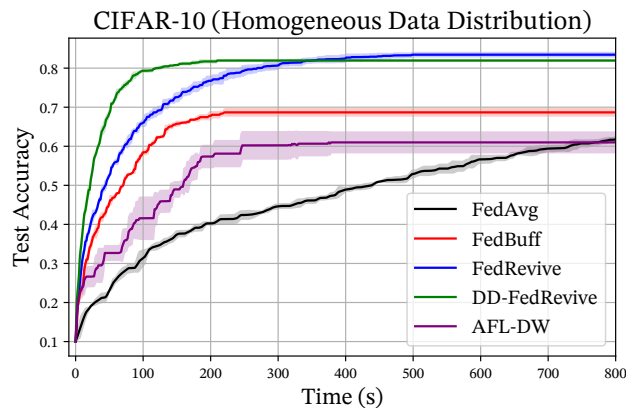


Figure 8: CIFAR-10 test accuracy with IID data partition.

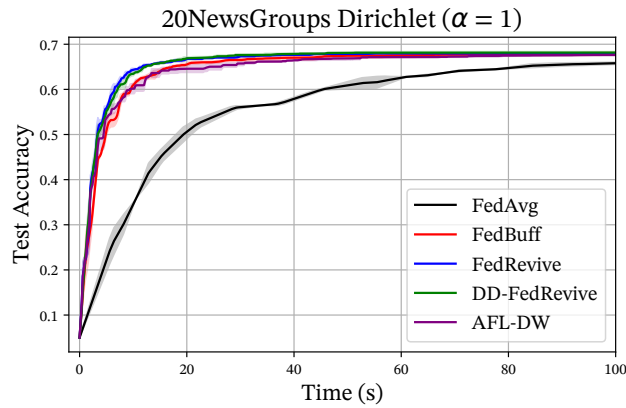


Figure 9: 20NewsGroups test accuracy over simulated time with $\alpha = 1$. FEDREVIVE achieves faster convergence than FEDBUFF.

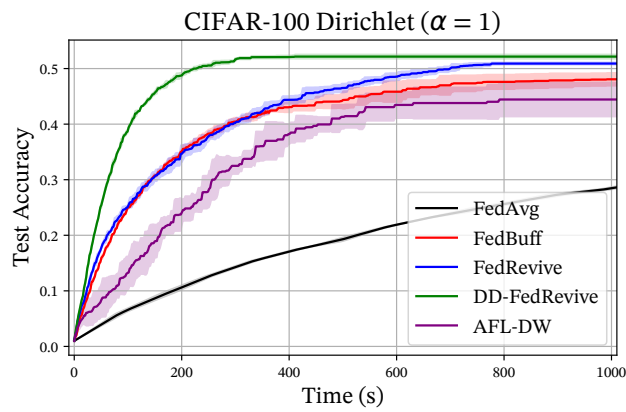


Figure 10: CIFAR-100 test accuracy over simulated time with $\alpha = 1$. FEDREVIVE consistently achieves higher final accuracy despite reduced heterogeneity.

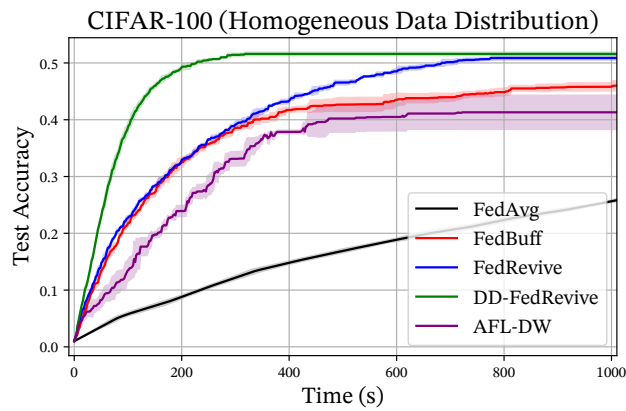


Figure 11: CIFAR-100 test accuracy under IID data distribution.

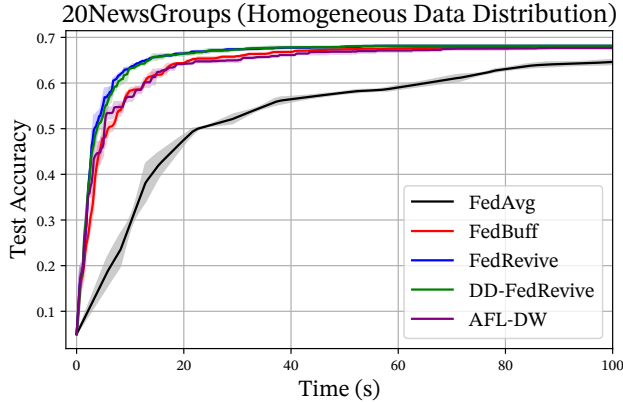


Figure 12: 20NewsGroups test accuracy under IID client partition.

B Raw Training Curves without Best-So-Far Processing

As described in the main text, asynchronous algorithms often display fluctuations in performance due to delayed updates and highly heterogeneous model aggregation. To provide a clearer comparison, the main figures report the *best-so-far* test accuracy over time. Here, we present the original unprocessed curves showing the raw test accuracy trajectories. Figures 13–16 illustrate these curves.

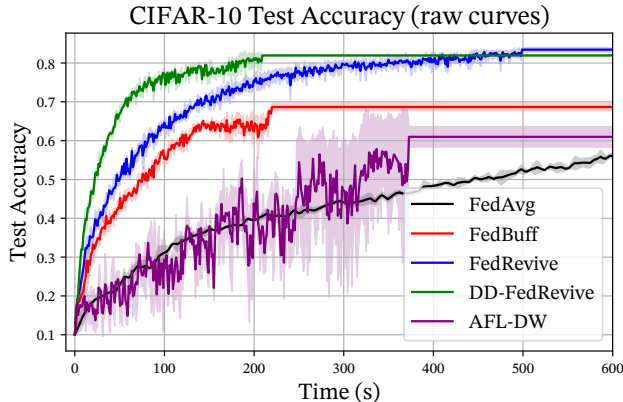


Figure 13: CIFAR-10 raw test accuracy curves.

C Does FedRevive Use Extra Memory?

At first glance, one might suspect that our proposed method introduces additional memory overhead on the server side, since the server needs to retain the previous version of the global model to compute the update step in Algorithm 1. This may raise the question of whether FEDREVIVE requires extra storage compared to standard asynchronous FL baselines.

In practice, this is not the case. In conventional FL, clients must also store a copy of the initial global model they receive before local training in order to compute their update $\Delta_i = \tilde{\mathbf{x}}_i - \mathbf{x}$ in the end of the local training. Thus, while FEDREVIVE performs this subtraction at the server rather than on the client, the memory cost is not increased. It is instead simply shifted from the client to the server. Since the server typically has substantially greater computational and memory capacity than edge clients, this shift has negligible impact in realistic deployments.

Moreover, this minor duplication can be further avoided altogether by performing the aggregation directly with

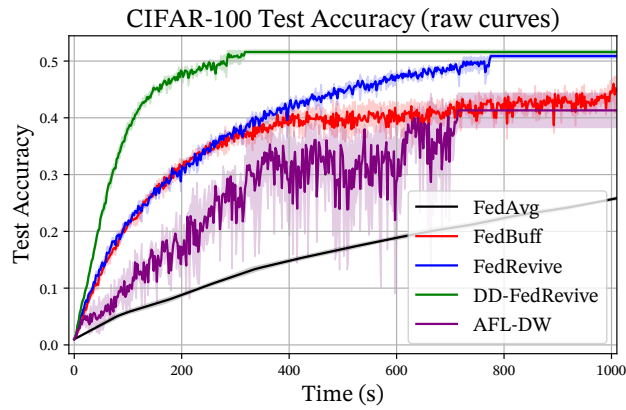


Figure 14: CIFAR-100 raw test accuracy curves.

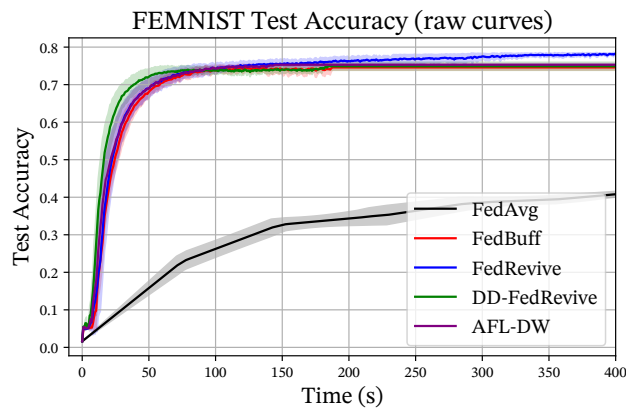


Figure 15: FEMNIST raw accuracy curves.

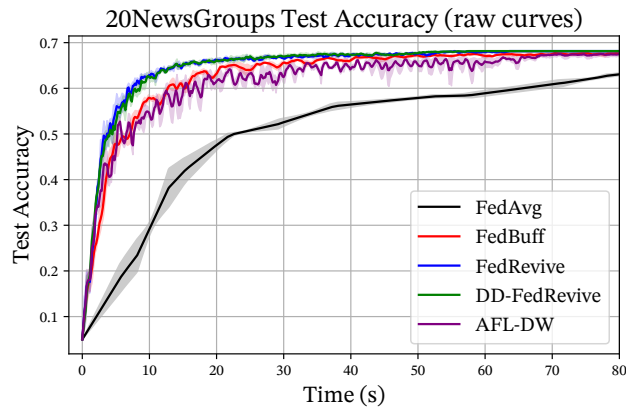


Figure 16: 20NewsGroups raw accuracy curves.

Table 2: Local and server learning rates used in each experiment.

Dataset	Method	η_c	η_s	Buffer Size
CIFAR-10	FEDAVG	0.0003	1.4	–
	FEDBUFF	0.0003	0.05	2
	AFL-DW	0.0003	0.1	–
	DD-FEDREVIVE	0.0003	0.2	–
	FEDREVIVE	0.0003	0.1	–
CIFAR-100	FEDAVG	0.0003	1.4	–
	FEDBUFF	0.0003	0.1	3
	AFL-DW	0.0003	0.1	–
	DD-FEDREVIVE	0.0001	0.3	–
	FEDREVIVE	0.0003	0.1	–
FEMNIST	FEDAVG	0.001	1.4	–
	FEDBUFF	0.001	0.025	1
	AFL-DW	0.001	0.05	–
	DD-FEDREVIVE	0.001	0.1	–
	FEDREVIVE	0.001	0.05	–
20NewsGroups	FEDAVG	0.003	1.0	–
	FEDBUFF	0.001	0.1	3
	AFL-DW	0.001	0.1	–
	DD-FEDREVIVE	0.001	0.1	–
	FEDREVIVE	0.001	0.1	–

Table 3: DFKD hyperparameters for each dataset.

Dataset	K_{KD} batch	K_{KD} batch	η	η_{synth}	η_{KD}
CIFAR-10	64	32	1e-4	0.001	0.003
CIFAR-100	64	32	3e-5	0.001	0.003
FEMNIST	64	32	1e-4	0.003	0.01
20NewsGroups	64	32	3e-4	0.1	0.01

the model parameters instead of the difference update. Specifically, instead of explicitly storing both \mathbf{x} and $\tilde{\mathbf{x}}_i$, the server can compute the aggregated model via a weighted interpolation:

$$\mathbf{x}^{(t+1)} = (1 - \eta_s) \mathbf{x}^{(t)} + \eta_s \tilde{\mathbf{x}}_i^{(t-\tau_i^t)},$$

for parameter-space aggregation with learning rate η_s but does not require forming or storing the explicit update vector. Consequently, FEDREVIVE introduces no additional memory overhead compared to standard vanilla FL.

D Experimental Details and Hyperparameters

We summarize the key hyperparameters used in all experiments below. All methods share the same training setup unless otherwise noted. For each dataset, we tune both client-side (*local*) and server-side (*global*) learning rates separately for each method, with AFL-DW using the same rates as FEDREVIVE. All models are trained with the Adam optimizer with momentum 0.9, local batch size 32, and 25 local iterations per client update. Validation and test splits are set to 0.15 of the total dataset each.

Client and Server Learning Rates. Table 2 lists the selected learning rates for all compared algorithms.

DFKD Settings. For FEDREVIVE, we use lightweight hyperparameters shared across all experiments unless otherwise stated. The distillation temperature T is fixed to 1. The KD buffer size, \mathcal{C} , is 8. Table 3 summarizes the task-specific parameters of the DFKD module.

The loss weights for the DFKD synthesis objective are consistent across datasets, with coefficients controlling the adversarial, feature-matching, and target alignment terms in Eq. 5: Adversarial Loss weight, $\alpha_{adv}=0.1$, Feature Loss weight, $\alpha_{feature} \in \{0.003, 0.0003, 0.3, 0.0001\}$, Target Loss weight, $\alpha_{target}=1.0$. Each value of Feature Loss weights corresponds to CIFAR-10, CIFAR-100, FEMNIST, and 20NewsGroups respectively.